WASHINGTON STATE DEPARTMENT OF
Natural Resources
Doug Sutherland - Commissioner of Public Lands
Division of Geology and Earth Resources
Ron Teissere - State Geologist

WASHINGTON DIVISION OF GEOLOGY AND EARTH RESOURCES
OPEN FILE REPORT 2004-9

Geologic Map of the Stimson Hill 7.5-minute Quadrangle, Skagit and Snohomish Counties, Washington

by Joe D. Dragovich, Michael W. Wolfe, Benjamin W. Stanton, and David K. Norman

June 2004

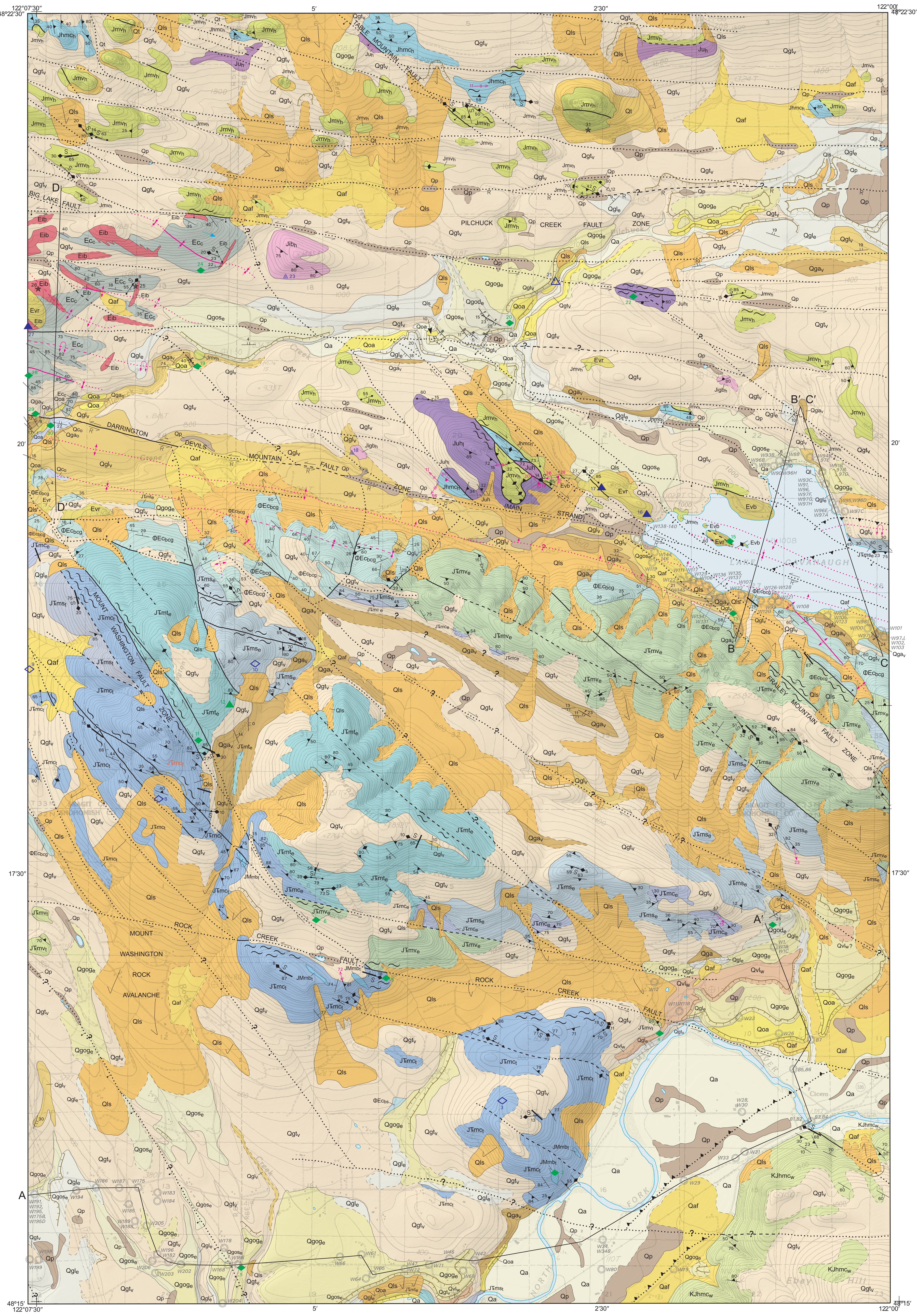

Lambert conformal conic projection
North American Datum of 1927; to place on North American Datum of 1983, move the projection lines 22 meters north and 92 meters east as shown by crosshair corner ticks
Base map from scanned and rectified U.S. Geological Survey 7.5-minute Stimson Hill quadrangle, 1985 (provisional edition); supplemented by additional contours on the northwest shore of Lake Cavanaugh from U.S. Geological Survey topographic survey of Lake Cavanaugh reservoir and dam sites, surveyed 1925, advance sheet printed 1926
Shaded relief generated from U.S. Geological Survey 10-meter Digital Elevation Model; vertical exaggeration 1.5x
Digital cartography by Anne C. Heinitz, Charles G. Caruthers, Sandra L. McAuliffe, and J. Eric Schuster
Editing and production by Karen D. Meyers

SCALE 1:24 000
1 MILE — 1000 7000 FEET — 1 KILOMETER
contour interval 40 feet

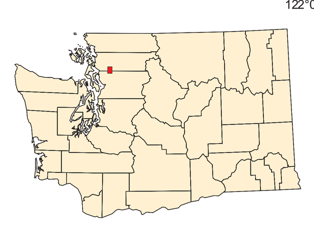

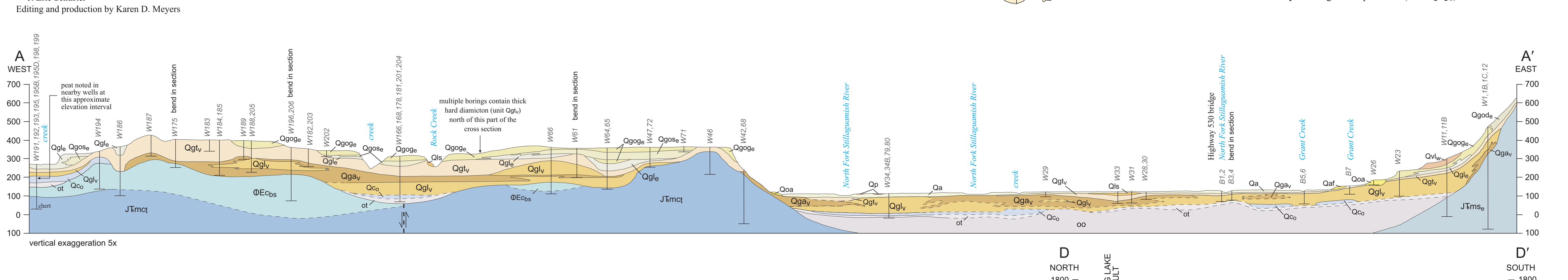

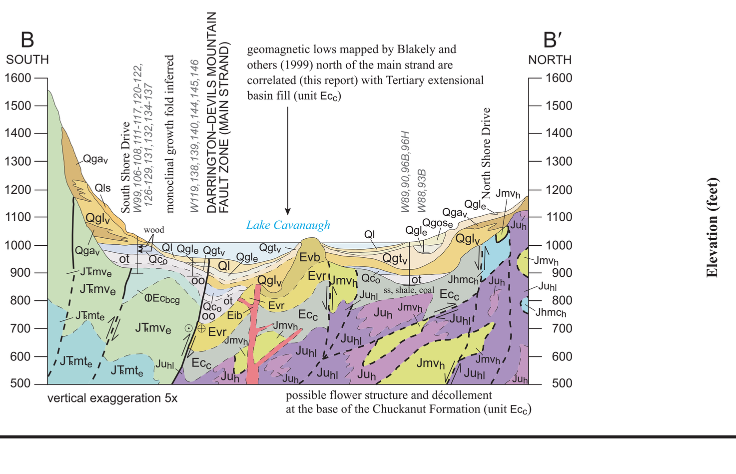

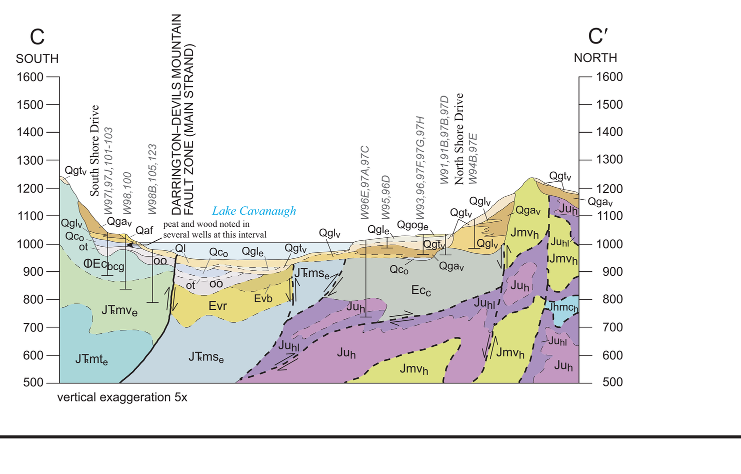

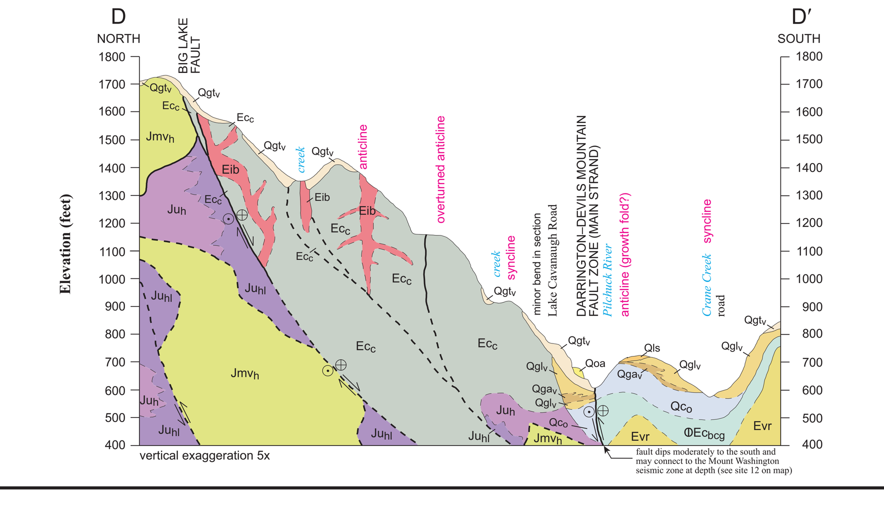

DESCRIPTION OF MAP UNITS

Information for the unit descriptions was compiled from the sources listed at the end of each description. The classification schemes we use are described in Dragovich and others (2002d). All measurements are given in English units with the exception of microscopic measurements, which are given in millimeters (1 mm = 0.04 in.).

Quaternary Sedimentary and Volcanic Deposits

HOLOCENE NONGLACIAL DEPOSITS

Qa — **Alluvium (Holocene)**—Channel deposits include sand, pebble gravel, and cobble gravel; gray; clasts are subrounded to rounded; loose, well stratified, and typically well sorted; plane-bedded sands common. North Fork Stillaguamish River gravels contain gray or reddish gray Glacier Peak dacite clasts (5–20%); other clasts are phyllite, slate, greenstone, volcanic rocks, granite, granite pegmatite, gneiss, vein quartz, schist, chert, conglomerate, sandstone, and siltstone. Pilchuck Creek alluvium consists mostly of sandy bouldery gravel with abundant greenstone.

Overbank deposits in the North Fork Stillaguamish River valley are mostly soft, grayish brown to olive-gray stratified sand, silt, clay, peat and muck deposits; thin (<25 ft)(cross section A). Several sticks obtained from peat beds in North Fork Stillaguamish River alluvium east of the study area yield radiocarbon ages of 2,270 and less than 600 yr B.P. (This study; Dragovich and others, 2002a,b, 2003b.)

Qp — **Peat (Holocene)**—Peat, organic sediment, and clay; mapped both in conspicuous abandoned channels within the North Fork Stillaguamish River and Pilchuck Creek floodplains and in poorly drained upland depressions containing marshes. Marshes locally contain thin beds of tephra from Mount Mazama (~6,900 yr B.P.). Many marshes occur along fault lineaments (this study; Dethier and others, 1980).

Qoa — **Older alluvium (Holocene)**—In the North Fork Stillaguamish River valley, consists of cobble gravel, sand, and pebble gravel with minor silt, forming terraces above the modern valley; gray and slightly oxidized to a red color; clasts are subrounded to rounded; loose; well sorted; clasts include greenstone, greenschist, granite, gneiss, schist, pumice, phyllite, slate, vein quartz, chert, quartzite, sandstone, siltstone, and minor Glacier Peak dacite (1–2%); 20 to 70 ft thick (cross section A).

Along Pilchuck Creek, best exposed at radiocarbon-age site 21 where it consists of a fining-upward sequence of basal greenstone-rich boulder-gravel lag overlain by interlayered pebbly sand, sand, and silty fine sand capped with interbedded peat, organic silt, and fine sand; underlain by scoured Vashon till 10 to 15 ft above river level; forms terraces separated from the creek by 20 to 55 ft high scarps that may have been stranded during Holocene tectonic uplift within the Darrington–Devils Mountain fault zone (DDMFZ). We obtained radiocarbon ages of 5,890 ±60 and 5,600 ±120 yr B.P. from twigs in the peat near the top of a terrace along Pilchuck Creek suggesting uplift of this terrace after about the mid-Holocene (site 21). Other poorly exposed terraces occur along the Pilchuck Creek in and west of the quadrangle (cross section D)(this study; J. D. Dragovich, Wash. Divn. of Geology and Earth Resources, unpub. data, 2003).

Qaf — **Alluvial fan deposits (Holocene)**—Debris-flow diamicton and alluvial sand and gravel; mostly poorly sorted; massive to weakly stratified; contains mostly angular to subangular, locally derived clasts. The distinction between units Qaf and Qls is at times difficult and differentiation relies on the lobate geomorphology of alluvial fans where streams enter open-valley settings. Some alluvial fans may have been initiated during late Pleistocene deglaciation. (This study; Dethier and others, 1980.)

Qls — **Landslide complexes (Holocene)**—Diamicton; contains locally derived angular to subangular clasts, but may contain some rounded clasts where sourced by Quaternary deposits; poorly sorted and unstratified; mostly includes slump–earthflows, debris slumps, debris flows, and rock avalanches. The large Mount Washington rock avalanche has 2.3 mi of run-out and may have been seismically induced. Some landslides may have initiated during late Pleistocene deglaciation. (This study; Dethier and others, 1980.)

Qt — **Talus deposits (Holocene)**—Poorly sorted angular gravel and sandy boulder gravel derived from exposed greenstone cliffs; includes rock-avalanche, rock-fall, and rockslide deposits.

Ql — **Lake deposits (Holocene)**—Sand, silt, and fine sand deposited in Lake Cavanaugh; overlies glaciolacustrine deposits; interfingers with units Qls and Qaf. We infer a maximum thickness of 55 ft (cross sections B, C). (This study; Naugler and others, 1996.)

LATE PLEISTOCENE GLACIER PEAK VOLCANIC DEPOSITS

Qvl$_w$ — **White Chuck assemblage of Beget (1981)**—Lahar deposits composed of noncohesive ashy pebbly sand and minor pumiceous alluvium; light reddish brown; compact; contains homogeneous dacite (67% SiO_2; site 4) and white pumice clasts up to 2 in.; dacite composes about 95 percent of the pebble and cobble component and is light to dark gray or weak red; dacite clasts are mostly subangular and vesicular; also contains rip-up clasts of glaciolacustrine clay up to 16 in. and rare clasts of White Chuck vitric tuff; symmetrically graded and 5 ft to 40 ft thick; caps an inset recessional outwash terrace 100 to 160 ft above the North Fork Stillaguamish River (cross section A). The White Chuck assemblage (~11,200–12,700 yr B.P.) resulted from Glacier Peak eruptions during deglaciation. (Beget, 1981; Dethier and others, 1980; Dragovich and others, 2002a,b,c,d; 2003a,b; J. D. Dragovich, Wash. Divn. of Geology and Earth Resources, unpub. data, 2000–2004.)

PLEISTOCENE GLACIAL AND NONGLACIAL DEPOSITS

Deposits of the Fraser Glaciation

Deposits of the Vashon Stade and Everson Interstade of the Fraser Glaciation blanket the map area. Vashon Stade continental ice advanced easterly up the North Fork Stillaguamish River and Deer Creek valleys about 15,500 yr B.P., blocking the major river valleys and forming temporary lakes in front of the advancing ice. Everson Interstade deglaciation commenced about 13,500 yr B.P., and the map area was probably fully deglaciated by about 11,500 yr B.P. (Armstrong and others, 1965; Pessl and others, 1989).

EVERSON INTERSTADE

In the map area, fluvial, deltaic, and lacustrine recessional deposits display lateral and vertical facies changes that are commonly gradational and interfingering. The provenance of fluvial and glaciolacustrine outwash sands differs between the North Fork Stillaguamish River and Pilchuck Creek recessional valley trains. Both have a mixed local, 'local-east' (from west-flowing meltwater drainages), and Canadian provenance. However, several thin sections of sand indicate that North Fork Stillaguamish River recessional outwash contains Glacier Peak dacite clasts (~3–5%, site 1), hornblende, hypersthene, as well as some high-grade metamorphic clasts from North Cascades sources significantly east of the area. Conversely, Pilchuck Creek recessional sands contain abundant clasts of local and 'local-east' provenance eroded from the Easton Metamorphic Suite and Helena–Haystack mélange. About 40 to 65 percent of clasts in Pilchuck Creek recessional outwash are phyllite, serpentinite, greenstone, listwaenite, greenschist, blue amphibole, and (or) blueschist (for example, site 20).

Qgog$_e$ — **Recessional outwash, gravel (Pleistocene)**—Pebbly sand and sandy pebble gravel, locally with cobbles; also contains thick to thin beds of sand, silty sand, and silt and a few rip-up clasts of glaciolacustrine clay; loose; subangular to subrounded clasts; generally forms subhorizontal beds a few feet thick that are crudely defined by variations in grain size; pebble imbrication, scour features, and cross-bedding indicate deposition in fluvial environments; directly overlies till (for example, site 1) or caps an overall upward-coarsening recessional stratigraphic section (cross sections A, B, C) that typically grades to former temporary glacial lake levels.

Qgod$_e$ — **Recessional outwash, deltaic (Pleistocene)**—Sandy cobble gravel, pebble gravel, pebbly sand, and sand; loose; moderately to well sorted; thin to very thickly bedded and well stratified; southerly dipping planar foreset beds 3 to 10 ft thick occur in sets 30 ft high or higher; delta at site 7 graded to a temporary, ice-dammed lake level of about 700 ft (cross section A); delta at site 20 (quarry) fines to bottomset beds of glaciolacustrine fine sand (unit Qgos$_e$) and then silt (unit Qgl$_e$) and is overlain by fluvial gravel topset beds (unit Qgog$_e$).

Qgos$_e$ — **Recessional outwash, sand (Pleistocene)**—Fine to medium sand, pebbly sand, and silty fine sand locally with thin interbeds of silt; loose; clasts are subangular to subrounded; nonbedded, plane bedded, laminated, or rarely cross-bedded; facies relations and fining trends suggest deposition in fluvial to mostly shallow-water glaciolacustrine settings; includes the Stillaguamish Sand Member of Vashon Drift in the southern part of the study area where the sand is mostly overlain by outwash gravel (unit Qgog$_e$) and underlain by or interbedded with finer-grained glaciolacustrine deposits (unit Qgl$_e$) (cross sections A, B).

Qgl$_e$ — **Recessional glaciolacustrine deposits (Pleistocene)**—Clay, silt, sandy silt, fine sand, and rare diamict; light gray to blue-gray weathered to shades of brown; well sorted; loose, soft, or stiff; nonbedded, laminated, or very thinly bedded with varves; locally contains flame and ball-and-pillow structures and rare sand dikes; common dropstone clast types include granite and greenstone; commonly interfingers with or underlies recessional outwash; deposited in glacial lakes impounded by receding glacial ice including glacial Lake Stillaguamish of Minard (1985) (near North Fork Stillaguamish River) and glacial Lake Pilchuck of this study (near Pilchuck Creek) (cross sections A, B, C).

VASHON STADE

Ice-flow indicators, sedimentary structures, and facies trends show that Puget lobe ice advanced over the map area from west-northwest to east-southeast. Advancing ice blocked the North Fork Stillaguamish River and Pilchuck Creek valleys, creating extensive ephemeral lakes. The resultant glaciolacustrine deposits are widespread and complexly interlayered with advance fluvial and deltaic deposits (cross sections A, B, C, D). Thin sections of sand show mixed Canadian and local provenance. Locally, however, sand composition and stratigraphic relations indicate that locally derived sand and gravel beds interfinger with Canadian-provenance detritus. This suggests that detritus entering temporary basins and lakes was deposited by both the advancing-ice meltwater and local, ice-free streams.

Qgt$_v$ — **Lodgment till (Pleistocene)**—Unstratified, matrix-supported clayey, silty, pebbly sand with disseminated cobbles and boulders; compact or dense; grayish blue to very dark gray and mottled yellowish brown to brownish gray; matrix commonly consists of silty sand or sandy silt with or without clay; includes Canadian-provenance and locally derived clasts; basal clasts are commonly excavated from underlying bedrock; rich in serpentinite and (or) greenstone clasts (up to 95%) where overlying the Helena–Haystack mélange, including some greenstone blocks up to about 80 ft wide; a carbonate-cemented 'till pavement' is common where till overlies serpentinite (unit Ju$_h$); generally 10 to 20 ft thick, but ranges from a discontinuous veneer to a 120 ft thick layer that mantles topography (cross sections A, B, C, D).

Qga$_v$ — **Advance outwash (Pleistocene)**—Medium to coarse sand, pebbly sand, and sandy pebble gravel with scattered beds of cobble gravel; locally contains fine sand, silt, and clay interbeds, flow till, and rare Mount St. Helens tephra (site 14); dense or compact; commonly well sorted; mostly moderately stratified and thinly to thickly bedded; cross-stratification, rip-up clasts of glaciolacustrine clay, and cut-and-fill structures common; deltaic foreset beds locally prominent; composite sections of units Qga$_v$ and Qgl$_v$ are up to 120 ft thick and locally crudely coarsen upward; primarily fluvial to locally deltaic; overlain by till along a sharp contact and conformably overlies or is complexly interlayered with unit Qgl$_v$ (cross sections A, B, C, D).

Qgl$_v$ — **Advance glaciolacustrine deposits (Pleistocene)**—Clay, silt, and silty clay with local dropstones; dropstone diamict commonly contains thin beds of laminated silt; locally contains thick beds of massive, clast-rich diamicton that may be flow till (or iceberg melt-out till); locally contains interbeds or lenses of medium to very thick beds of fine sandy silt, sand, and gravel; blue gray or gray, weathered to yellowish brown; stiff or dense; varies from massive to thinly bedded, laminated, or varved; soft-sediment and (or) ice-shear deformational features include contorted bedding, overturned folds, and flame structures. Overturned fold geometry is consistent with east-southeast-directed ice shear during ice advance up the major river valleys. This unit is locally underlain by unit Qc$_o$ and locally overlain by, and (or) interbedded with, unit Qga$_v$ (cross sections A, B, C, D). Sites 13 and 19 are well-exposed examples of very thickly interbedded deltaic or glaciofluvial advance outwash (unit Qga$_v$), dropstone diamicton, and glaciolacustrine clays.

Deposits of the Olympia Nonglacial Interval

Qc$_o$ — **Olympia beds of Armstrong and others (1965) (Pleistocene)**—Boulder gravel, cobble gravel, pebble gravel, sand, silt, clay, peat, and minor diamicton; very compact, well sorted, and very thin to thick bedded; disseminated organic material, logs, or wood fragments are common; iron-stained fluvial boulder gravel lag, cobble and pebble gravel, and sand deposits (site 30) contain abundant greenstone, serpentinite, and pyroxenite derived locally from the Helena–Haystack mélange; located immediately south of the main strand of the DDMFZ. Petrographic comparisons of sands at this site with nearby modern Pilchuck Creek alluvium indicate that both have similar composition (for example, 15–25% ultramafite and 5–10% greenstone). Using compositional and stratigraphic criteria, we correlate this alluvium with the Olympia beds (cross section D). Dragovich and others (2003a) obtained ages of 38,560 ±640 and 35,040 ±450 yr B.P. from Olympia beds adjacent to the DDMFZ main strand east of the study area. Generally, unit Qc$_o$ forms a dissected pre-Vashon stratum in the subsurface (cross section A) that is inferred to be gently folded and tectonically uplifted south of the main strand of the DDMFZ (cross sections B, C, D).

Pre-Fraser Glacial Deposits

ot — **Older till (Pleistocene) (cross sections only)**—Clay, silt, sand, and gravel in various proportions, with scattered cobbles and boulders; correlation with the Possession Glaciation is tentative. We do not assign a formal geologic symbol to this unit to emphasize the tentative nature of this correlation with Possession Glaciation.

oo — **Older outwash (Pleistocene) (cross sections only)**—Sand, gravel, silt, clay, and diamicton; sand and gravel directly below unit ot may correspond to the Possession outwash; also includes undivided pre-Possession glacial or nonglacial sediments below the inferred outwash. We do not assign a formal geologic symbol to this unit to emphasize the tentative nature of this correlation with Possession Glaciation.

Tertiary Intrusive, Volcanic, and Sedimentary Rocks

Although controversial, we follow Tabor and others (2002) and correlate the volcanic rocks in the study area with the Barlow Pass Volcanics. (Compare Tabor and others, 2002, and Evans and Ristow, 1994.) Regionally, Barlow Pass Volcanics consist of a diverse rhyolite, andesite, dacite, and basalt suite with local dikes and nonmarine sedimentary interbeds. Volcanic rocks in the map area are a bimodal rhyolite–basalt suite preserved in extensional or transtensional basins of the DDFMZ. Regional and local ages suggest that these volcanic rocks are early middle Eocene to the earliest Oligocene. Volcanic rocks mostly overlie the volcanic-lithic-poor lower Eocene Coal Mountain unit of the Chuckanut Formation (Evans and Ristow, 1994). Regionally, the Coal Mountain unit generally lacks volcanic interbeds, in contrast to the younger Chuckanut units, which locally contain significant amounts of volcanic lithic clasts, bentonites, and other indicators of proximal to distal volcanic deposition.

VOLCANIC AND HYPABYSSAL INTRUSIVE ROCKS

Eib — **Diabase (Eocene)**—Homogeneous, medium-grained, subophitic basaltic diabase dikes and sills; contains euhedral, randomly oriented blocky plagioclase (0.2–2 mm; 50–55%), subhedral augite (0.2–1 mm; 25–30%), distinctive bladed opaque minerals (4–5%), and interstitial quartz (0–2%) in an altered matrix (~10%) of brown chlorite and rare carbonate; dark greenish gray; intrudes the Chuckanut Formation at several localities (cross section D). Bechtel, Inc. (1979) obtained whole-rock K-Ar ages of 46.4 ±2.2 (site 25), 41.2 ±1.8 (site 26), and 49.9 ±2.2 Ma (site 26). The petrographic similarity of the diabase dikes with unit Evb suggests that the dikes may be feeders for the nearby basalt flows. (This study; Dethier and others, 1980.)

Evb — **Basalt (Eocene)**—Basalt flows; contains euhedral microlites and blocks of plagioclase (0.05–2 mm; 40–60%), opaque minerals (8%), interstitial quartz (0–1%), and glass (5–40%) mostly altered to brown chlorite (20%); greenish gray; contains trachytic flow textures and flow-aligned chlorite-carbonate-filled vesicles; basalt near trachytic diabase at site 15 displays flow-aligned vesicles to 1 in. long. (See unit Eib.)

Evr — **Rhyolite (Eocene)**—Thick flows, breccias, dikes, and ash flows (vitric tuff ±lapilli) of high-silica rhyolite; contains scattered quartz ±plagioclase ±sanidine phenocrysts in a glassy matrix; quartz is microlitic to 2 mm; smoky quartz varies from euhedral to anhedral and locally resorbed; plagioclase (up to 2 mm) is euhedral to subhedral; glass (up to 90%) is spherulitic and partly highly altered; clasts are mostly pumice lapilli and xenoliths and xenocrysts of the Chuckanut Formation; secondary minerals include chlorite, sericite, orthoclase, and vesicle-filling chalcedony; rhyolite is bluish to greenish gray weathered to shades of yellow, red, or white; locally contains porphyritic and trachytic textures, stretched vesicles, flow banding, and flattened pumice fiamme. Whetten and others (1988) obtained zircon fission-track ages of 43.5 ±2.2 (site 16), 38.1 ±1.8 (site 17), and 52.7 ±2.5 Ma (site 27). The latter site is from a rhyolite dike that intrudes the Chuckanut Formation, although Whetten and others (1988) suggest that the rhyolite is interbedded with the Chuckanut rocks as a tuff or flow. Six other ages (35.2–45.1 Ma) near the study area suggest volcanism extended into the earliest Oligocene. (This study; Lovseth, 1975; Tabor and others, 2002; Dragovich and others, 2002a,b, 2003a,b.)

SEDIMENTARY ROCKS

ΦEc$_{bcg}$, ΦEc$_{bs}$ — **Rocks of Bulson Creek of Lovseth (1975) (Oligocene to Eocene)**—Conglomerate with local interbeds and lenses of pebbly sandstone, chert-lithic sandstone, and siltstone; rare boulder conglomerate lag; poorly cemented; greenish gray weathered to yellowish brown; clasts are subangular to subrounded, subspherical to elongate with abundant (meta)chert; may be crudely imbricated and normally graded; thick interbeds of sandstone vary from massive to graded with channeling and cross-bedding locally observed; fines to the south to include interbedded fluvial to shallow-marine sandstone, siltstone, and coal (unit ΦEc$_{bs}$ in cross section A); locally unconformably overlies and contains clasts derived from the Eastern mélange belt and Trafton sequence (with only minor Helena–Haystack mélange detritus); deposited directly south of the main strand of the DDMFZ in fluvial and alluvial-fan basin(s). Lovseth (1975) and Marcus (1981) report late Eocene to early Oligocene shallow-water marine fossils in the unit west of the map area. Bulson Creek sandstones are volcanolithic west of the study area (Frizzell, 1979; Dragovich and others, 2002c) indicating that deposition may have been influenced by nearby Eocene to Oligocene volcanism.

Ec$_c$ — **Coal Mountain unit of Evans and Ristow (1994) of the Chuckanut Formation (Eocene)**—Fluvial feldspathic sandstone with less-abundant conglomerate, shale, siltstone, and coal; sandstone is light gray and weathered to yellowish brown; micaceous; medium to coarse grained; sandstone–shale ratio is about 3:1; thick to very thin bedded; well sorted; clasts are rounded to subrounded; coarse-grained beds contain trough cross-bedding and ripple or plane laminations; fine-grained beds contain ripples, flutes, load casts, and plant fossils. Several sites (for example, sites 24 and 28) have a high potassium-feldspar (7–25%) and low lithic-clast content (3–8%), which is consistent with the Coal Mountain unit provenance regionally. Regional plant-fossil ages and ages of volcanic rocks that are intrusive into or overlying the unit indicate an early Eocene age (>49–52 Ma)(cross section D). (This study; Whetten and others, 1988; Frizzell, 1979.)

Mesozoic to Paleozoic Low-Grade Metamorphic Rocks (Prehnite–Pumpellyite to Blueschist Facies)

HELENA–HAYSTACK MÉLANGE

The Helena–Haystack mélange of Tabor (1994) is a serpentinite-matrix mélange. Resistant blocks of greenstone erode out of mélange matrix as steep hillocks. Regional greenstone geochemistry suggests a mid-oceanic-ridge to oceanic-island-arc ophiolitic origin. Whetten and others (1980, 1988) obtained U-Pb zircon ages of 160 to 170 Ma (Jurassic) from greenstone in and outside the map area (see sites 18 and 23). Questionable K-Ar (uplift?) plagioclase, pyroxene, and whole rock ages near and in the study area vary from 125 Ma (site 31) to 164 Ma (Bechtel, Inc., 1979). Mélange formation is likely mid-Cretaceous. However, Tertiary deformation within the DDMFZ has significantly increased the fault imbrication of tectonic blocks in the map area (cross sections B, C, D). (Dragovich and others, 2002b,c,d, 2003a,b; Tabor, 1994; Tabor and others, 2002.)

Jmv$_h$ — **Greenstone (Jurassic)**—Metamorphosed basalt with minor andesite, dacite, and rare rhyolite occurring as flows and less-abundant tuff; relict phenocrysts include augite, saussuritized plagioclase, and rare hornblende; metamorphic minerals include albite, chlorite, acicular actinolite, Fe- and Mg-pumpellyite, prehnite, stilpnomelane, aragonite, and calcite; grayish green and weathered to dark greenish gray to yellowish brown; flows locally contain amygdules, breccia, and pillows; commonly non- to weakly foliated but locally contains strong spaced cleavage; fractured, veined, or mylonitized near faults (this study; Tabor and others, 2002).

Jigb$_h$ — **Metagabbro (Jurassic)**—Medium-grained to rarely coarse-grained uralitic greenstone; rare hornblende-biotite meta–quartz diorite to fine-grained quartz amphibolite gneiss; relict minerals include saussuritized and albitized plagioclase, augite or pigeonite, brown actinolized hornblende, and minor interstitial quartz; metamorphic minerals include acicular actinolite, tremolite, epidote, chlorite, pumpellyite, white mica, stilpnomelane, calcite, and (or) aragonite; metamorphic recrystallization typically static; light to dark greenish gray weathered to yellowish or grayish brown; hypidiomorphic-granular with ophitic or subophitic relict igneous textures; generally nonfoliated, but weakly foliated to protomylonitic near faults.

Ju$_h$ — **Ultramafite (Jurassic)**—Serpentinite and less-abundant talc-tremolite rock with minor partially serpentinized dunite, peridotite, and pyroxenite; composed mostly of serpentine minerals such as antigorite, locally with relict pyroxene and (or) olivine and accessory picotite, magnesite, and opaque minerals including chromite; serpentinite is greenish gray to greenish black and weathered to a dark yellowish orange; massive to strongly foliated; locally grades to silica-carbonate rock (unit Ju$_{hl}$).

Ju$_{hl}$ — **Silica-carbonate rocks (Jurassic)**—Silica-carbonate mineralization products (listwaenites) resulting from metasomatism of ultramafites; contains pods of incompletely altered serpentinite and brecciated silica-carbonate rock; minerals include microcrystalline quartz and magnesite in roughly equal amounts, with magnesite forming aggregates and vein swarms; magnetite, pyrite, and marcasite occur as accessory minerals; locally contains talc, tremolite, and chlorite; vugs contain quartz with overgrowths of dolomite; commonly displays compositionally banded veins or replacement bands of quartz, magnesite, chalcedony, and dolomite; brown to orange-brown weathered to a reddish or brownish yellow; metasomatism causes the unusual occurrence of resistant ridges along fault zones (for example, ridge at site 22). Some metasomatism is clearly associated with hydrothermal alteration along DDMFZ. Elsewhere, metasomatism may have been driven by hydrothermal alteration around Eocene intrusive bodies (cross sections B, D). (This study; Dragovich and others, 2002b,c, 2003a,b.)

Jhmc$_h$ — **Heterogeneous metamorphic rocks, chert bearing (Jurassic)**—Medium-gray phyllitic meta-argillite, bluish gray metasandstone, and metashale and metachert; weathered bluish or dark greenish gray; metamorphic minerals are chlorite, white mica, epidote, graphite, and lawsonite; locally well stratified and very thinly bedded; phyllite characterized by a strong S1 (first-generation) phyllitic to slaty cleavage with local F2 (second-generation) folds, L2 crenulations, and F3 (third-generation) kinks; most rocks very thinly bedded from meta-argillite to metasandstone; bedding subparallel to the S1 cleavage in F1 fold limbs and nonparallel in fold hinges.

WESTERN AND EASTERN AND MÉLANGE BELTS AND THE TRAFTON SEQUENCE

The Western and Eastern mélange belts of Tabor and others (2002) are submarine-fan to deep-oceanic deposits. Volcanic sandstone provenance and the occurrence locally of tuff and flow interbeds are suggestive of near-volcanic-edifice deposition. This is consistent with the basalt geochemistry, which consistently indicates an intraplate seamount (hotspot) setting. Prehnite–pumpellyite facies assemblages are widespread in the belts. The probable lack of metamorphic aragonite suggests that the belts have not undergone the high-pressure metamorphism typical of the Northwest Cascades system. Although both belts have an argillite–phyllite mélange matrix, the Eastern mélange belt is less foliated than the Western belt. The Trafton sequence of Danner (1966) is likely correlative with the Eastern mélange belt, and both have been thrust over the Western belt. Furthermore, both belts may originally have been thrust over rocks of the Northwest Cascades system. However, Tertiary fault rejuvenation in the DDMFZ has largely modified primary Cretaceous thrust-fault contacts in the map area. (This study; Tabor, 1994; Tabor and others, 2002; Whetten and others, 1988.)

Rocks of the Western Mélange Belt

KJhmc$_w$ — **Heterogeneous metamorphic rocks, chert-bearing (Cretaceous–Jurassic)**—Semischistose lithofeldspathic to volcanolithic subquartzose metasandstone, slate, phyllite, locally abundant metachert, and rare limestone; also contains greenstone derived from mafic volcanic breccia, tuff, and flows locally with pillows and vesicles; metasandstone clasts include rip-up clasts of argillite, angular to subrounded plagioclase, monocrystalline and polycrystalline quartz, chert, volcanic lithic fragments, and mica; metamorphic minerals are carbonate, prehnite, pumpellyite, chlorite, epidote, and sericite; commonly medium- to thick-bedded with rhythmite and laminate bedding, graded bedding, and load casts locally well preserved; typically moderately to strongly foliated. Radiolarians in metachert and megafossils in meta-argillite southeast of the map area indicate that the belt (excluding limestone) is Late Jurassic to earliest Cretaceous. Limestone blocks (olistostromes?) southeast of the study area are Permian. (Tabor and others, 2002; Dragovich and others, 2003b.)

Rocks of the Eastern Mélange Belt

JTrmt$_e$ — **Mixed metavolcanic and metasedimentary rocks, undivided (Jurassic–Triassic)**—Metamorphosed volcanic lithofeldspathic sandstone, argillaceous sandstone (wacke), siltstone, argillite, chert, and minor thin tuff; non- to weakly foliated; prehnite common in veins; cataclastic and protomylonitic near the Rock Creek and Mount Washington fault zones (for example, site 11). (This study; Tabor and others, 2002; Dethier and others, 1980.)

JTrmv$_e$ — **Greenstone (Jurassic–Triassic)**—Metamorphosed plagioclase- and augite-bearing basalt, basaltic andesite, and andesite; metamorphic minerals include epidote, pumpellyite, prehnite, and chlorite; dark to greenish gray or dusky green weathered to dark greenish or bluish gray; may contain very thick beds of light bluish gray, medium-grained volcanic feldspatholithic metasandstone; consists of mostly porphyritic to aphanitic thick flows with breccia and minor thinner beds of augite-bearing tuff; local amygdaloidal flow tops and pillows; massive to rarely incipiently foliated; cataclastic, pervasively fractured, and locally protomylonitic near fault zones on Frailey Mountain. Augite-bearing metabasalt at site 6 is interpreted as an intraplate alkaline basalt based on geochemical signature. (This study; Dethier and others, 1980; Tabor, 1994; Tabor and others, 2002.)

JTrms$_e$ — **Metasedimentary rocks (Jurassic–Triassic)**—Metamorphosed argillite, lithofeldspathic to feldspatholithic sandstone, wacke, and siltstone with minor chert, tuffaceous greenstone, and chert pebble conglomerate; argillite commonly contains radiolarians and scattered silt-sized grains of angular quartz and plagioclase; sand-sized grains in sandstone and wacke are volcanic- and (or) chert-rich and also contain angular to subrounded plagioclase, monocrystalline and polycrystalline quartz, quartz-mica tectonite, mica, sedimentary lithic fragments including coarse rip-up clasts of argillite, and rare coral and granitic fragments; metamorphic minerals include epidote, chlorite, pumpellyite, calcite, and white mica; prehnite typically occurs in veins; rocks vary from massive to incipiently foliated to moderately fracture cleaved; foliated and protomylonitic near faults; northeast vergence suggested by a F1-folded metachert on Frailey Mountain. Whetten and others (1988) obtained Late Jurassic radiolarians from metachert (site 10). (This study; Dethier and others, 1980; Tabor and others, 2002.)

JTrmc$_e$ — **Metachert (Jurassic–Triassic)**—Metamorphosed radiolarian-bearing chert and cherty argillite locally with interbedded argillite, siltstone, and fine-grained sandstone; chert is black and very thinly bedded to ribboned with thin laminae of argillite; weakly foliated, locally folded, and protomylonitic near faults; veins of quartz common; radiolarians from chert southeast of the study area are Triassic and Jurassic (this study; Tabor and others, 2002; Dethier and others, 1980). (See units JMmb$_t$ and JTrmc$_t$ for a discussion of the ages of the likely correlative Trafton sequence.)

Trafton Sequence of Danner (1966)

The Trafton sequence is a mélange and is likely correlative with the Eastern mélange belt. Fossils in the Trafton sequence range from Mississippian to Early Jurassic. Whetten and others (1988) report Early Triassic and early and middle Pennsylvanian conodonts from pods and tectonic blocks of limestone near the study area (two sites west of site 9). A large body of metatonalite at least as old as Pennsylvanian occurs in the Trafton adjacent to the map area (directly southwest of site 9). In addition, Danner (1966) has identified Permian Tethyan fusulinids in limestone pods south of the study area. Regionally, Trafton metacherts yield radiolarian ages mostly ranging from Triassic to Jurassic. The generally Mesozoic age of the Trafton metacherts contrasts with the mostly Paleozoic age of Trafton limestones and suggests that the limestone bodies are partly olistostromal.

JTrmc$_t$ — **Metachert (Jurassic–Triassic)**—Metamorphosed chert and cherty argillite interbedded locally with argillite, siltstone, and minor thin beds of carbonaceous shale, wacke, and tuff; chert contains micro- and polycrystalline quartz (88–95%), chlorite (3–6%), disseminated organic material (2–5%), and white mica (0–1%); chert is banded red, black, and gray and is very thin bedded to ribboned with thin laminae of argillite, less commonly occurring as thin laminae in meta-argillite; weakly foliated and locally complexly boudinaged and folded; protomylonitic, chloritized, fractured, and veined near faults; veins of quartz common. The geometry of boudins, vein arrays, S-C fabric, and lineations in protomylonitic chert at three sites near the Rock Creek fault (for example, site 5) indicate left-lateral strike-slip fault motion. Whetten and others (1988) obtained partially recrystallized Triassic radiolarians from metachert in the map area (sites 3 and 8) and Middle Jurassic radiolarians from near the study area (west of site 9). (This study; Tabor and others, 2002; Dethier and others, 1980.) (Also see age information for unit JMmb$_t$.)

JTrms$_t$ — **Metasedimentary rocks (Jurassic–Triassic)**—Metamorphosed argillite, siltstone, fine-grained feldspatholitic sandstone, chert, cherty argillite, and tuff; angular to subrounded sandstone clasts are volcanic and (or) chert-rich and also contain plagioclase, monocrystalline and polycrystalline quartz, quartz-mica tectonite, mica, and sedimentary lithic fragments including rip-up clasts of argillite; metamorphic minerals include epidote, chlorite, pumpellyite, prehnite, calcite, and white mica; rocks vary from non- to incipiently foliated or moderately fracture cleaved; protomylonitic, cataclastic, and brecciated near faults. (This study; Dethier and others, 1980.)

JTrmv$_t$ — **Greenstone (Jurassic–Triassic)**—Metabasalt; contains phenocrysts of plagioclase and clinopyroxene; metamorphic minerals include chlorite and pumpellyite; contains carbonate and quartz veins; contains amygdules and forms pillows or massive flows. (This study; Dethier and others, 1980.)

JMmb$_t$ — **Marble (Jurassic–Mississippian)**—Marble and limestone; locally contains interbeds of metamorphosed ribbon chert and argillite; calcite extensional veins pervasive; dark gray, bluish gray or black; forms a series of elongate, steeply dipping lenticular bodies (20–50 ft thick). The limestone quarry at site 2 exposes a steeply dipping, lenticular marble with partially faulted contacts. However, the occurrence of calcareous shale in the surrounding metachert implies that a gradational stratigraphic contact exists between the limestone and the surrounding chert host rocks (unit JTrmc$_t$). Also, the limestone is not internally disrupted and therefore was not likely emplaced tectonically or as an olistostrome. These observations suggest that the limestones in the map area are similar in age to unit JTrmc$_t$ and are thus likely Mesozoic. (This study; Danner, 1966; Tabor and others, 2002.)

DARRINGTON–DEVILS MOUNTAIN FAULT ZONE

The Darrington–Devils Mountain fault zone (DDMFZ) divides the Northwest Cascades system on the north from the Eastern and Western mélange belts on the south (Tabor, 1994) and is a regional structure (Dragovich and others, 2002b,c,d; Tabor, 1994). The DDMFZ initiated as a broad strike-slip fault zone that is over 8 mi wide in the map area. It has a complex displacement history beginning at the mid-Eocene (or perhaps the mid-Cretaceous) and continuing to recent times (Johnson and others, 2001).

Dragovich and others (2002c, 2003a,b) modeled the Tertiary fault zone as a flower structure within an overall left-lateral transpressional fault regime with many en echelon fault segments and imbricate tectonic blocks. We envision a similar deformational style for the current study area (cross sections B, C, D). Right-lateral strike-slip antithetic faults such as the Mount Washington and Frailey Mountain fault zones are subparallel to northwest-trending en echelon fold axes. These elements merge with the left-lateral main strand of the DDMFZ and subparallel master faults such as the Rock Creek, Pilchuck Creek, and Big Lake fault zones. Field and microscopic examination of boudins, extensional veins, and S-C intersections in areas containing steeply dipping cataclasite or protomylonite with shallow slickenlines indicate largely strike-slip kinematics within these fault zones (for example, sites 5, 11, 13 and 22).

There was no obvious active DDMFZ faulting during the open-basin deposition of the Coal Mountain unit. However, younger Chuckanut Formation units near the study area have a local provenance and sedimentary structures indicative of active strike-slip faulting along the DDMFZ and development of regional tectonic partitioning during the early middle Eocene. Fault truncation of the Coal Mountain unit, tight folding, and emergence of the mélange belts south of the fault occurred during this time. Mélange-belt emergence suggests strike-slip faulting with an oblique *south-side-up* component producing transpressional uplift of highlands. The synchronous initiation of early middle Eocene volcanism, preserved in local transtensional basins, likely accompanied this change to closed basins and local emergent landmass geometry around the map area. Later Eocene to Oligocene deposition of the rocks of Bulson Creek only south of the DDMFZ main strand suggests oblique *south-side-down* transtensional strike-slip faulting. Strike-slip-generated folding waned at this time (this study; Evans and Ristow, 1994; Tabor and others, 2002).

Regional tectonic data and earthquake focal mechanisms indicate that the DDMFZ is likely currently under almost pure north–south compression (Ma and others, 1996; Zollweg and Johnson, 1989; Van Wagoner and others, 2002). Zollweg and Johnson (1989) defined the active Darrington seismic zone directly east of the study area using a local portable seismometer array. Their hypocenter and focal-mechanism geometry implies an active *south-side-up* thrust fault zone striking N80°W ±20°, dipping south at 40° ±15°, with a strike length of at least 6 to 12 mi. Similarly, Van Wagoner and others (2002) reported two earthquake clusters of focal-mechanism data consistent with north-south compression on the DDMFZ to the east of the map area. Dragovich and others (2003a,b) correlated the Darrington seismic zone hypocenter data and Pacific Northwest Seismic Network data with the DDMFZ main strand to the east (cross section C of Dragovich and others, 2003a) and inferred that the main strand shallows southward into a gently south-dipping regional décollement. In the present map area, the Mount Washington seismic zone (around site 12) includes a tight cluster of 39 recent earthquakes (magnitude 1.9–3.1, depth of 1.4–8.8 mi), recorded in the Advanced National Seismic System hosted by the Northern California Earthquake Data Center, that may be downdip of the main strand reverse fault.

The map distribution of Holocene and Pleistocene deposits suggests that lower stratigraphic levels have been uplifted along and south of the DDMFZ main strand and implies *south-side-up* reverse faulting of the DDMFZ main strand. For example, laharic valley fills thin abruptly east of the map area, south of where the DDMFZ crosses the North Fork Stillaguamish River area, indicating south-side-up Holocene uplift and erosion after about 5 ka (Dragovich and others, 2002a,b, 2003a,b). The valley also contains uplift-related(?) older alluvial terraces and shallow Vashon glacial deposits (cross section A). Also, this uplift is further supported by the anomalous exposures of Olympia beds directly south of the main strand (site 30 and cross section D), Olympia beds at a shallow stratigraphic depth along the south shore of Lake Cavanaugh (cross section B, C), erosion and removal of Everson recessional deposits along and south of the main strand, and Vashon advance lake and outwash deposits high along the flanks of Frailey Mountain (for example, site 13). (Also see Dragovich and others, 2003a, 2002c, and Adair and others, 1989, for Olympia beds possibly uplifted along the DDMFZ main strand east and west of the map area.)

Additional evidence for Holocene uplift in the DDMFZ includes uplifted river terraces along Pilchuck Creek north of the main strand (see unit Qoa). Radiocarbon-dated peat from an inset Holocene terrace suggests mid-Holocene or younger uplift for at least this portion of the area (site 21). Similar uplifted terraces occur along the Pilchuck Creek to the west (cross section D). Based on these terraces as well as map pattern and geomorphic anomalies, we infer that fault strands within the Pilchuck Creek fault zone are locally active and may sole into the DDMFZ décollement at depth (this study; Dragovich and others, 2002a,b,c, 2003a,b; J. D. Dragovich, Wash. Divn. of Geology and Earth Resources, unpub. data, 2000–2004).

Further evidence for Holocene DDMFZ activity includes: (1) probable displacement of Vashon glacial strata along the main strand east of the map area (site 8 of Dragovich and others, 2003b) and likely tectonic deformation of Vashon glacial deposits directly south of the main strand in the map area (site 29); (2) liquefaction features in glacial sediments; (3) increased landslide density near the DDMFZ; and (4) deformation of Holocene and late-glacial recessional lake sediments at the bottom of Lake Cavanaugh defined using a high-resolution seismic survey that imaged about 10 to 16 ft of vertical offset (Naugler and others, 1996) (cross section B, C). Although the seismic profile is unpublished, Naugler and others (1996) suggest that our units Ql and Qgl$_e$ have been folded and faulted in the Holocene and that the DDFMZ main strand has about 3 to 5 m of vertical offset. They emphasize Holocene strike-slip offset versus our inference that the main strand has largely reverse offset in the Holocene.

ACKNOWLEDGMENTS

This report was produced in cooperation with the U.S. Geological Survey National Cooperative Geologic Mapping Program Agreement Number 03HQAG0086. We thank Ryan Bradley for exceptional field assistance; Diane Johnson and Charles Knaack (Wash. State Univ.) for geochemical sample analysis; Jeff Jones (Snohomish County) for providing geotechnical-boring logs; Rowland Tabor (U.S. Geological Survey emeritus) for enlightening discussions; and Washington Division of Geology and Earth Resources staff members Bill Lingley for landslide information, Josh Logan and Tim Walsh for map reviews, and Tara Salzer for clerical support.

Disclaimer: This product is provided 'as is' without warranty of any kind, either expressed or implied, including, but not limited to, the implied warranties of merchantability and fitness for a particular use. The Washington Department of Natural Resources will not be liable to the user of this product for any activity involving the product with respect to the following: (a) lost profits, lost savings, or any other consequential damages; (b) the fitness of the product for a particular purpose; or (c) use of the product or results obtained from use of the product. This product is considered to be exempt from the Geologist Licensing Act [RCW 18.220.190 (4)] because it is geological research conducted by the State of Washington, Department of Natural Resources, Division of Geology and Earth Resources.

GEOLOGIC SYMBOLS

- Contact—Dashed where inferred and (or) location poorly known
- Fault, unknown offset—Dashed where inferred; dotted where concealed; queried where uncertain
- Normal fault—Bar and ball on downthrown side; dotted where concealed; queried where uncertain
- Reverse fault—R on upthrown side; dashed where inferred; dotted where concealed
- Strike-slip fault—Arrows show apparent relative motion; dashed where inferred; dotted where concealed
- Oblique-slip fault—Bar and ball on downthrown side; arrows show apparent relative lateral motion; dotted where concealed; queried where uncertain
- Reverse and strike-slip fault—R on upthrown side; arrows show apparent relative lateral motion; dashed where inferred; dotted where concealed. We suspect that the main strand of the Darrington–Devils Mountain fault zone has Tertiary left-lateral and (or) oblique offset and Quaternary reverse offset (see section on Darrington–Devils Mountain fault zone in text)
- Thrust fault—Sawteeth on upper plate; dotted where concealed
- Monocline, anticlinal bend—Concealed; queried where uncertain
- Anticline—Dashed where inferred; dotted where concealed
- Overturned anticline—Dashed where inferred; dotted where concealed
- Syncline—Dashed where inferred; dotted where concealed
- Late Pleistocene to Holocene terrace or landslide scarp—Hachures point downslope
- Direction of landslide movement
- Inclined bedding—Showing strike and dip
- Vertical bedding—Showing strike
- Overturned bedding—Showing strike and dip
- Inclined bedding in unconsolidated sedimentary deposits—Showing strike and dip; F near symbol indicates foreset bedding; B indicates bottomset bedding
- Inclined foliation in metamorphic rock—Showing strike and dip
- Vertical or near-vertical foliation in metamorphic rock—Showing strike
- Inclined mylonitic folation—Showing strike and dip
- Minor inclined fault—Showing strike and dip
- Minor vertical or near-vertical fault—Showing strike
- Minor second-generation fold axial surface—Showing strike and dip
- Extensional vein—Showing strike and dip
- Inclined slickensided fracture surface—Showing strike and dip
- Vertical slickensided fracture surface—Showing strike
- Minor first-generation (F1) fold axis—Showing bearing and plunge
- Minor second-generation (F2) fold axis or crenulation lineation—Showing bearing and plunge
- Minor third-generation (F3) fold axis or kink or crenulation lineation—Showing bearing and plunge
- Slip lineation or slickenside on a fault or shear surface—Showing bearing and plunge of offset
- Stretching lineation—Showing bearing and plunge
- Current flow direction indicator (pebble imbrication, ripples, etc.)—Showing bearing and plunge
- Glacial striae—Showing bearing
- Mylonitic or cataclastic shear zone
- Radiocarbon age (this study)(site 21, sample 03-40P)
- Whole rock K-Ar radiometric age (Bechtel, Inc., 1979)
- Zircon U-Pb-Th age (R. E. Zartman *in* Whetten and others, 1988; Whetten and others, 1980)
- Zircon fission-track age (C. W. Naeser *in* Whetten and others, 1988)
- Microfossil age (D. L. Jones *in* Whetten and others, 1988)
- Center of area of high seismicity within the Mount Washington seismic zone. Zone is defined using hypocenter information from the on-line Advanced National Seismic System, hosted by Northern California Earthquake Data Center (http://quake.geo.berkeley.edu/anss/catalog-search.html) and is a possible westward extension of the Darrington seismic zone of Zollweg and Johnson (1989)
- Important sites with well-exposed geologic relationships, geochemical analyses, structure, or representative thin sections (see text)
- Water well or geotechnical borehole used in cross sections—W indicates water well; B indicates geotechnical borehole; number is assigned by authors (see cross sections for numbers)

CROSS SECTIONS ONLY

- Strike-slip motion on fault—Bullseye shows apparent relative fault motion toward viewer; cross symbol shows apparent relative fault motion away from viewer
- Dip-slip motion on fault—Arrows show apparent relative motion

REFERENCES CITED

Adair, M. J.; Talmage, R. H.; Crosby, T. W.; Testa, S. M., 1989, Geology and seismicity of the Skagit Nuclear Power Plant site. *In* Galster, R. W., chairman, Engineering geology in Washington: Washington Division of Geology and Earth Resources Bulletin 78, v. I, p. 607-624.

Armstrong, J. E.; Crandell, D. R.; Easterbrook, D. J.; Noble, J. B., 1965, Late Pleistocene stratigraphy and chronology in southwestern British Columbia and northwestern Washington: Geological Society of America Bulletin, v. 76, no. 3, p. 321-330.

Bechtel, Inc., 1979, Report of geologic investigations in 1978-1979; Skagit Nuclear Power Project: Puget Sound Power and Light Company, 3 v., 3 plates.

Beget, J. E., 1981, Postglacial eruption history and volcanic hazards at Glacier Peak, Washington: University of Washington Doctor of Philosophy thesis, 192 p.

Blakely, R. J.; Wells, R. E.; Weaver, C. S., 1999, Puget Sound aeromagnetic maps and data: U.S. Geological Survey Open-File Report 99-514, version 1.0 [accessed Oct. 3, 2000 at http://geopubs.wr.usgs.gov/open-file/of99-514/]

Danner, W. R., 1966, Limestone resources of western Washington; with a section on the Lime Mountain deposit, by G. W. Thorsen: Washington Division of Mines and Geology Bulletin 52, 474 p.

Dethier, D. P.; Whetten, J. T.; Carroll, P. R., 1980, Preliminary geologic map of the Clear Lake SE quadrangle, Skagit County, Washington: U.S. Geological Survey Open-File Report 80-303, 11 p., 2 plates.

Dragovich, J. D.; Gilbertson, L. A., Lingley, W. S., Jr.; Polenz, Michael; Glenn, Jennifer, 2002a, Geologic map of the Darrington 7.5-minute quadrangle, Skagit and Snohomish Counties, Washington: Washington Division of Geology and Earth Resources Open File Report 2002-7, 1 sheet, scale 1:24,000.

Dragovich, J. D.; Gilbertson, L. A., Lingley, W. S., Jr.; Polenz, Michael; Glenn, Jennifer, 2002b, Geologic map of the Fortson 7.5-minute quadrangle, Skagit and Snohomish Counties, Washington: Washington Division of Geology and Earth Resources Open File Report 2002-6, 1 sheet, scale 1:24,000.

Dragovich, J. D.; Gilbertson, L. A.; Norman, D. K.; Anderson, Garth; Petro, G. T., 2002c, Geologic map of the Utsalady and Conway 7.5-minute quadrangles, Skagit, Snohomish, and Island Counties, Washington: Washington Division of Geology and Earth Resources Open File Report 2002-5, 1 sheet, scale 1:24,000.

Dragovich, J. D.; Logan, R. L.; Schasse, H. W.; Walsh, T. J.; Lingley, W. S., Jr.; Norman, D. K.; Gerstel, W. J.; Lapen, T. J.; Schuster, J. E.; Meyers, K. D., 2002d, Geologic map of Washington—Northwest quadrant: Washington Division of Geology and Earth Resources Geologic Map GM-50, 3 sheets, scale 1:250,000, with 72 p. text.

Dragovich, J. D.; Stanton, B. W.; Lingley, W. S., Jr.; Griesel, G. A.; Polenz, Michael, 2003a, Geologic map of the Mount Higgins 7.5-minute quadrangle, Skagit and Snohomish Counties, Washington: Washington Division of Geology and Earth Resources Open File Report 2003-12, 1 sheet, scale 1:24,000.

Dragovich, J. D.; Stanton, B. W.; Lingley, W. S., Jr.; Griesel, G. A.; Polenz, Michael, 2003b, Geologic map of the Oso 7.5-minute quadrangle, Skagit and Snohomish Counties, Washington: Washington Division of Geology and Earth Resources Open File Report 2003-11, 1 sheet, scale 1:24,000.

Evans, J. E.; Ristow, R. J., Jr., 1994, Depositional history of the southeastern outcrop belt of the Chuckanut Formation—Implications for the Darrington–Devil's Mountain and Straight Creek fault zones, Washington (U.S.A.): Canadian Journal of Earth Sciences, v. 31, no. 12, p. 1727-1743.

Frizzell, V. A., Jr., 1979, Point count data and sample locations for selected samples from Paleogene nonmarine sandstones, Washington: U.S. Geological Survey Open-File Report 79-293, 31 p., 2 plates.

Johnson, S. Y.; Dadisman, S. V.; Mosher, D. C.; Blakely, R. J.; Childs, J. R., 2001, Active tectonics of the Devils Mountain fault and related structures, northern Puget Lowland and eastern Strait of Juan de Fuca region, Pacific Northwest: U.S. Geological Survey Professional Paper 1643, 45 p., 2 plates.

Lovseth, T. P., 1975, The Devils Mountain fault zone, northwestern Washington: University of Washington Master of Science thesis, 29 p.

Ma, Li; Crosson, R. S.; Ludwin, R. S., 1996, Western Washington earthquake focal mechanisms and their relationship to regional tectonic stress. *In* Rogers, A. M.; Walsh, T. J.; Kockelman, W. J.; Priest, G. R., editors, Assessing earthquake hazards and reducing risk in the Pacific Northwest: U.S. Geological Survey Professional Paper 1560, v. 1, p. 257-283.

Marcus, K. L., 1981, The rocks of Bulson Creek—Eocene–Oligocene sedimentation and tectonics in the Lake McMurray area, Washington: Western Washington University Master of Science thesis, 84 p., 1 plate.

Minard, J. P., 1985, Geologic map of the Arlington East quadrangle, Snohomish County, Washington: U.S. Geological Survey Miscellaneous Field Studies Map MF-1739, 1 sheet, scale 1:24,000.

Naugler, W. E.; Karlin, R. E.; Holmes, M. L., 1996, Lakes as windows in the crust—Lake Cavanaugh and the Devils Mountain fault, northwestern Washington [abstract]: Geological Society of America Abstracts with Programs, v. 28, no. 5, p. 95.

Pessl, Fred, Jr.; Dethier, D. P.; Booth, D. B.; Minard, J. P., 1989, Surficial geologic map of the Port Townsend 30- by 60-minute quadrangle, Puget Sound region, Washington: U.S. Geological Survey Miscellaneous Investigations Series Map I-1198-F, 1 sheet, scale 1:100,000, with 13 p. text.

Tabor, R. W., 1994, Late Mesozoic and possible early Tertiary accretion in western Washington State—The Helena–Haystack mélange and the Darrington–Devils Mountain fault zone: Geological Society of America Bulletin, v. 106, no. 2, p. 217-232, 1 plate.

Tabor, R. W.; Booth, D. B.; Vance, J. A.; Ford, A. B., 2002, Geologic map of the Sauk River 30- by 60-minute quadrangle, Washington: U.S. Geological Survey Geologic Investigations Series Map I-2592, 2 sheets, scale 1:100,000, with 67 p. text.

Van Wagoner, T. M.; Crosson, R. S.; Creager, K. C.; Medema, G. F.; Preston, L. A.; Symons, N. P.; Brocher, T. M., 2002, Crustal structure and relocated earthquakes in the Puget Lowland, Washington, from high-resolution seismic tomography: Journal of Geophysical Research, v. 107, no. B12, 2381, DOI:10.1029/20012JB000710, p. ESE 22-1 - 22-23.

Whetten, J. T.; Carroll, P. I.; Gower, H. D.; Brown, E. H.; Pessl, Fred, Jr., 1988, Bedrock geologic map of the Port Townsend 30- by 60-minute quadrangle, Puget Sound region, Washington: U.S. Geological Survey Miscellaneous Investigations Series Map I-1198-G, 1 sheet, scale 1:100,000.

Whetten, J. T.; Zartman, R. E.; Blakely, R. J.; Jones, D. L., 1980, Allochthonous Jurassic ophiolite in northwest Washington: Geological Society of America Bulletin, v. 91, no. 6, p. I 359-I 368.

Zollweg, J. E.; Johnson, P. A., 1989, The Darrington seismic zone of northwestern Washington: Seismological Society of America Bulletin, v. 79, no. 6, p. 1833-1845.